Cell, Vol. 112, 113–122, January 10, 2003, Copyright ©2003 by Cell Press

Crystal Structure of Carnitine Acetyltransferase and Implications for the Catalytic Mechanism and Fatty Acid Transport

Gerwald Jogl and Liang Tong*
Department of Biological Sciences
Columbia University
New York, New York 10027

Summary

Carnitine acyltransferases have crucial roles in the transport of fatty acids for β-oxidation. Dysregulation of these enzymes can lead to serious diseases in humans, and they are targets for therapeutic development against diabetes. We report the crystal structures of murine carnitine acetyltransferase (CRAT), alone and in complex with its substrate carnitine or CoA. The structure contains two domains. Surprisingly, these two domains share the same backbone fold, which is also similar to that of chloramphenicol acetyltransferase and dihydrolipoyl transacetylase. The active site is located at the interface between the two domains. Carnitine and CoA are bound in deep channels in the enzyme, on opposite sides of the catalytic His343 residue. The structural information provides a molecular basis for understanding the catalysis by carnitine acyltransferases and for designing their inhibitors. Specifically, our structural information suggests that the substrate carnitine may assist the catalysis by stabilizing the oxyanion in the reaction intermediate.

Introduction

Carnitine acyltransferases catalyze the exchange of acyl groups between carnitine and coenzyme A (CoA) (Bieber, 1988; Kerner and Hoppel, 2000; McGarry and Brown, 1997; Ramsay et al., 2001). These enzymes include carnitine acetyltransferase (CRAT, also known as CAT), carnitine octanoyltransferase (COT), and carnitine palmitoyltransferase (CPT), with substrate preferences for short chain, medium chain, and long chain fatty acids, respectively. These enzymes generally contain about 600 residues, with molecular weights of about 70 kDa (Figure 1).

The carnitine acyltransferases have important biological functions. CPT-I and CPT-II are crucial for the β-oxidation of long chain fatty acids in the mitochondria, by facilitating their transport across the mitochondrial membrane (McGarry and Brown, 1997; Ramsay et al., 2001). The activity of CPT-I is inhibited by malonyl-CoA, a crucial regulatory mechanism for fatty acid oxidation (Abu-Elheiga et al., 2001). CRAT may be involved in the transport of acetyl-CoA across intracellular membranes, in maintaining the acetyl-CoA:CoA balance, and in the excretion of excess or harmful acyl molecules as acylcarnitines (Bieber, 1988; Ramsay et al., 2001). CRAT activity may also be required for progression through G1 to the S phase of the cell cycle (Brunner et al., 1997).

Mutation or dysregulation of these enzymes have been linked to many serious, even fatal human diseases. Inherited recessive defects of CPT-I and CPT-II can give rise to hypoketonemia and hypoglycemia, with severely reduced blood glucose levels (McGarry and Brown, 1997; Ramsay et al., 2001). CPT-II deficiency is the most common cause of abnormal lipid metabolism in skeletal muscle, including muscle pain and myoglobinuria (DiMauro and Melis-DiMauro, 1973). Both single-point mutations and insertions/deletions in these genes have been observed to produce the clinical phenotype. Inherited deficiency in CRAT activity can lead to serious neurological and heart problems, and patients suffering from Alzheimer's disease also have reduced CRAT activity (Brunner et al., 1997).

Carnitine acyltransferases are promising targets for the development of therapeutic agents against several human diseases. Inhibitors of L-CPT-I, an isoform of CPT-I that is mostly expressed in liver, kidney, and fibroblasts, are efficacious for the treatment of non-insulin-dependent diabetes mellitus (NIDDM) (Anderson, 1998; Giannessi et al., 2001; Ramsay et al., 2001; Wagman and Nuss, 2001), where disrupted glucose levels are caused at least in part by increased fatty acid oxidation. A covalent inhibitor of L-CPT-I, etomoxir, can lower blood glucose levels in diabetic animals and humans, demonstrating the feasibility of this type of inhibitors. The clinical applications of such irreversible inhibitors are unfortunately severely limited by their toxic side effects. The design and development of new, reversible inhibitors of L-CPT-I has so far been a rather challenging process (Anderson, 1998), and better understanding of the structure and function of these enzymes is needed.

However, currently there is no structural information on any of these transferases. Crystals of human CRAT have recently been reported (Lian et al., 2002). Moreover, there is no recognizable sequence homology between these enzymes and other proteins in the database. To understand the molecular mechanism for the catalysis by this important family of enzymes and to provide a structural basis for the identification of their inhibitors, we have determined the crystal structure of mouse CRAT, alone and in complex with the substrate carnitine or CoA, at up to 1.8 Å resolution. The amino acid sequences of the various carnitine acyltransferases are significantly conserved among the eukaryotes (Figure 1), with murine CRAT sharing about 35% amino acid sequence identity to the other enzymes. Our structural observations on CRAT should therefore be generally applicable to this entire family of enzymes.

Results and Discussion

Structure Determination

The crystal structure of the free enzyme of mouse CRAT was determined at 1.8 Å resolution by the selenomethionyl single-wavelength anomalous diffraction (SAD) method (Hendrickson, 1991). There are two molecules of the protein in the crystallographic asymmetric unit, and each molecule contains 21 methionine residues (ex-

*Correspondence: tong@como.bio.columbia.edu

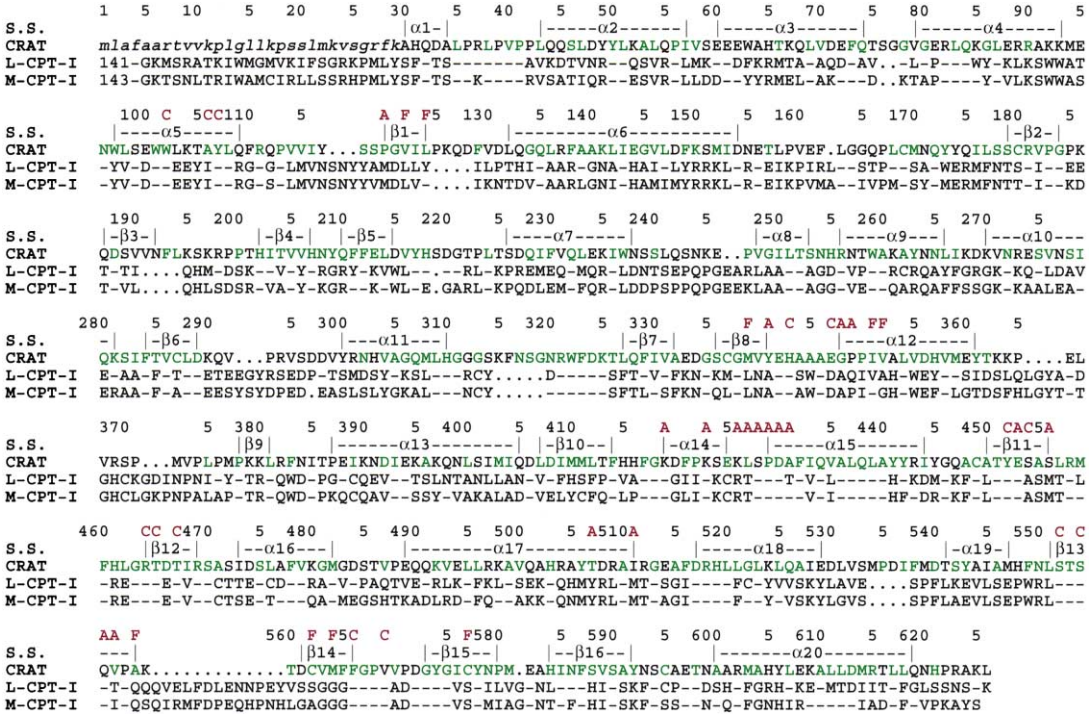

Figure 1. Sequence Alignment of Mouse Carnitine Acetyltransferase (CRAT) and Human Liver- and Muscle-Type Carnitine Palmitoyltransferase I (L-CPT-I and M-CPT-I).

The secondary structure elements in the CRAT structure are labeled (S.S.). Residues shown in green are in the core of the protein, with less than 25% exposed surface area. Residues in the carnitine (C), CoA (A), and fatty acid (F) binding pockets are also indicated. The residue numbers are for CRAT. An additional 140 residues at the N terminus of L-CPT-I and M-CPT-I are not shown. A dash represents a residue that is identical to that in CRAT, while a dot represents a deletion.

cluding the initiator Met). A total of 40 Se sites were located based on the anomalous differences, and our structural analysis showed that the Met residue near the N terminus of each protein molecule is disordered. This Met residue is present only in the recombinant protein, introduced as a part of the His-tag by the expression vector. The N-terminal His-tag is disordered in the crystal.

To determine the binding mode of the substrate carnitine or CoA, we produced crystals of mouse CRAT in the presence of these compounds. The subsequent structural analysis at 1.9 Å resolution defined the binding mode of carnitine in the active site, but showed the binding of oxidized CoA to the "wrong" region of the active site. In these CoA crystals, the thiol of CoA was oxidized to a sulfonic acid, even in the presence of 10 mM DTT in the crystallization solution. The sulfonic group of oxidized CoA is bound in the pocket that recognizes the carboxylate group of carnitine, supporting the preference for a negatively charged group in that pocket. The ADP portion on the other end of the CoA molecule is disordered.

The binding mode of CoA was determined instead from an X-ray diffraction data set on a free enzyme crystal soaked with acetyl-CoA. The crystal suffered serious damage during the soaking process, and the quality of the diffraction data set is rather poor (Table 1). Consequently, the *R* factor for the atomic model is high (Table 1). Nonetheless, the binding mode of CoA is clearly defined by the electron density map.

The molecules in the asymmetric unit of these crystals have essentially the same conformation, with rms distance of 0.34 Å for 587 equivalent Cα atoms. The contacts among the non-crystallographically related and the crystallographically related dimers in these crystals are generally weak and hydrophilic in nature. The protein migrates as monomers on gel filtration columns (data not shown). The structural observations are consistent with biochemical data suggesting that the protein is monomeric in solution (Ramsay et al., 2001).

Overall Structure of CRAT

The crystal structure of the free enzyme of mouse CRAT has been determined at 1.8 Å resolution. The current atomic model contains residues 30–625 for each of the two molecules in the asymmetric unit, which essentially corresponds to the full-length, mature form of this enzyme. All the residues except Ile116 are located in favored regions of the Ramachandran plot. Ile116 is the second residue in a type II reverse turn, and its main chain conformation is clearly defined by the electron density. The crystallographic information is summarized in Table 1.

The structure of CRAT contains 16 β strands (β1–β16) and 20 α helices (α1–α20) and can be divided into two domains (Figure 2A). The C domain contains a six-stranded mixed β sheet, together with eleven α helices. Residues in this domain include the C-terminal 1/3 of the protein (residues 407–626) as well as residues 30–95 at the N terminus, which contribute four α helices to this

Table 1. Summary of Crystallographic Information

Substrate	—	Carnitine	CoA
Maximum resolution (Å)	1.8	1.9	2.3
Number of observations	749,015	347,562	135,285
R_{merge} (%)[1]	4.4 (12.0)	5.7 (17.4)	8.8 (26.1)
I/σI	19.1 (6.2)	19.6 (6.7)	9.5 (3.2)
Resolution range used for refinement	30–1.8 Å	20–1.9 Å	30–2.3 Å
Number of reflections[2]	235,313	105,409	53,398
Completeness (%)	97 (94)	97 (93)	85 (75)
R factor (%)[3]	18.8	20.1	27.0
Free *R* factor (%)	21.7	24.1	36.3
rms deviation in bond lengths (Å)	0.005	0.006	0.009
rms deviation in bond angles (°)	1.2	1.2	1.3

[1] $R_{merge} = \sum_h \sum_i |I_{hi} - \langle I_h \rangle| / \sum_h \sum_i |I_{hi}|$. The numbers in parentheses are for the highest resolution shell.
[2] The number for the free enzyme includes both Friedel pairs.
[3] $R = \sum_h |F_h^o - F_h^c| / \sum_h F_h^o$.

domain and interact with a segment between α17 and β13 (Figure 2B). One face of the β sheet in this domain is covered by the α helices, whereas part of the other face of this sheet contacts the N domain of the structure (residues 96–385). Helix α13, residues 386–487, forms the long connection between the N and the C domains (Figure 2A).

The N domain contains an eight-stranded mixed β sheet, which is covered on both sides by eight α helices (Figure 2C). This eight-stranded β sheet is formed by

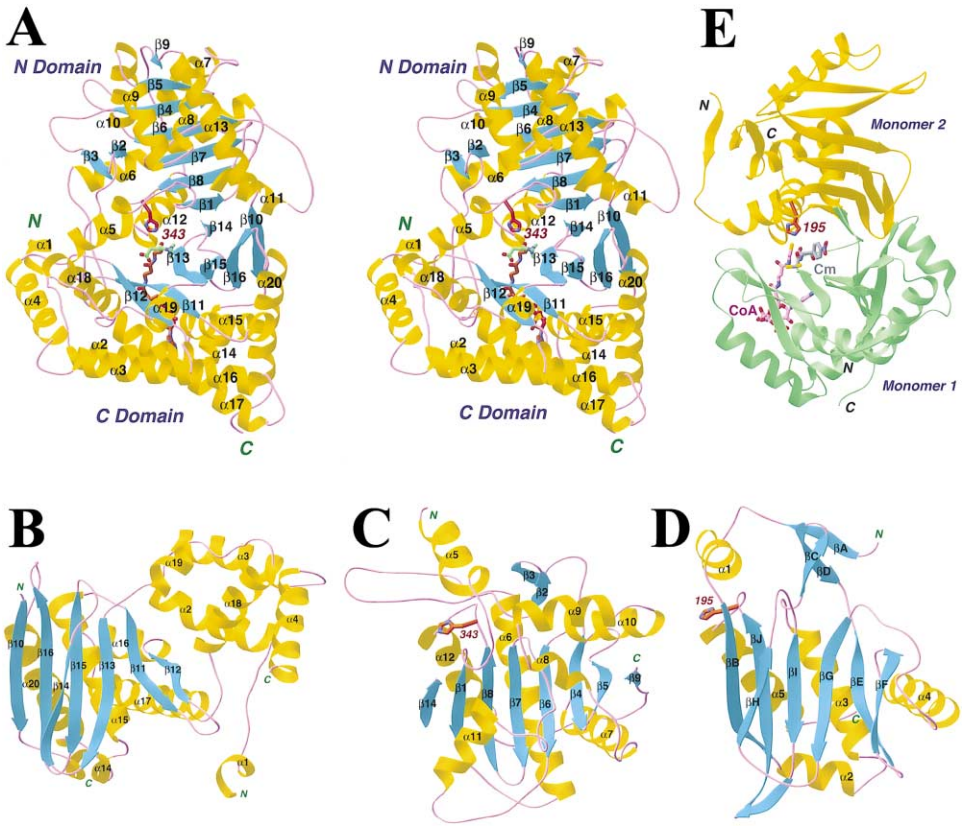

Figure 2. Structure of CRAT

(A) Stereo diagram showing a schematic representation of the structure of CRAT. The β strands and α helices are labeled, and the catalytic His343 residue is shown in red. The binding modes of carnitine (in green) and CoA (in brown) are also indicated.
(B) Structure of the C domain of CRAT.
(C) Structure of the N domain of CRAT, in the same orientation as the C domain.
(D) Structure of the monomer of chloramphenicol acetyltransferase CAT, viewed in the same orientation as (B). The secondary structure elements are named according to Leslie et al., 1988. The catalytic His195 residue is shown in red.
(E) Structure of two monomers in the trimer of CAT. The active site is located at the interface between the two monomers. The substrates CoA and chloramphenicol (Cm) are also shown and labeled. Produced with Ribbons (Carson, 1987).

flanking the central six-stranded sheet with one extra β strand on each of its edges (Figure 2C). Interestingly, one of these extra β strands actually comes from the C domain. Part of the β13–β15 crossover connection in the C domain forms a β strand (β14) (Figure 2B), and this strand is hydrogen-bonded to β1 in an anti-parallel fashion in the N domain (Figure 2C). The N domain also contains a pair of β strands (β2 and β3) on the surface, helping enclose one end of the β sheet.

Surprisingly, the N and C domains share very similar polypeptide backbone folds (Figures 2B and 2C), despite the lack of any recognizable amino acid sequence homology between them. This structural homology is limited to the core of the two domains, including the central six β strands of the β sheet and three α helices closely associated with it (α6, α7, and α12 in the N domain). A total of 71 Cα positions can be superimposed to within 3.5 Å of each other between the two domains, and the rms distance for these equivalent atoms is 2.0 Å. However, there are only three pairs of identical residues (4%) among these structurally aligned positions, underscoring the lack of amino acid sequence conservation between the two domains.

Unexpected Structural Conservation with Chloramphenicol Aetyltransferase (CAT) and Dihydrolipoyl Transacetylase (E2pCD)

Comparisons with the protein structure database, performed with the program Dali (Holm and Sander, 1993), revealed that the N and the C domains of CRAT have similar backbone folds as that of chloramphenicol acetyltransferase (CAT) (Figure 2D) (Leslie et al., 1988) and the catalytic domain of dihydrolipoyl transacetylase (E2pCD) (Mattevi et al., 1992). Both of these enzymes catalyze the transfer of an acetyl group from acetyl-CoA to an organic substrate. In addition, E2p forms the cubic core of the pyruvate dehydrogenase multienzyme complex (Mattevi et al., 1992). A total of 161 out of 213 Cα atoms in CAT can be superimposed with the equivalent atoms in the C domain of CRAT, and the rms distance of these atoms is 3.7 Å. The amino acid sequence identity among these structurally equivalent residues is however only 9%. Similar observations are made when the CAT structure is aligned with the N domain of CRAT or when the structure of E2pCD is used for comparison.

Most remarkably, the structural conservation between CRAT and CAT or E2pCD extends beyond the similarity in their backbone folds. The organization of the two domains of CRAT is similar to that of two monomers in the trimers of CAT and E2pCD (Figure 2E). The rotational relationship between the N and C domains of CRAT is 118°, close to a 3-fold rotation. Both CAT and E2pCD function as trimers, and the active site of the enzymes is located at the interface between a pair of monomers in the trimer (Figure 2E) (Leslie et al., 1988; Mattevi et al., 1992). It appears that CRAT may have evolved by gene duplication of a single-domain enzyme (such as E2p or CAT), and the resulting two-domain enzyme has the same function as a homo-trimer of the single-domain enzymes.

The amino acid sequences of CRAT have diverged significantly from those of CAT and E2pCD. In addition, the N and C domains of CRAT contain about 300 amino acid residues each, larger than the sizes of CAT and E2pCD (about 220 residues). As a result, the two domains in CRAT have significant insertions in several of the surface loops as compared to CAT or E2pCD (Figures 2B–2D). These insertions form additional interactions within the domains, for example those between the α18–α19 insertion and helices α2–α4 in the C domain (Figure 2B). In the N domain, the α8–α10 and α11 insertions cover the face of the β sheet (Figure 2C) that would be shielded from solvent by the third monomer in the trimers of CAT and E2pCD.

The Active Site of CRAT

Previous biochemical, kinetic, and mutagenesis studies have identified a histidine residue, equivalent to His343 in CRAT (Figure 1), as the catalytic residue for the carnitine acyltransferases (McGarry and Brown, 1997; Ramsay et al., 2001). Our structural analysis confirms the functional importance of the His343 residue, in the connection between β8 and α12 in the N domain (Figure 2C). It is located at the same position as His195 in CAT (Figure 2D) and His610 in E2pCD, the catalytic residues of these enzymes (Leslie et al., 1988; Mattevi et al., 1992). As in CAT and E2pCD, the side chain of the His343 residue in CRAT is held in an unusual conformation, such that the Nδ1 ring nitrogen in the side chain is hydrogen-bonded to the carbonyl oxygen in its main chain.

The active site of CRAT is located deep in the enzyme, at the interface between the N and C domains (Figure 2A). The His343 residue can be reached by two separate channels, of 15–18 Å depth each, from opposite sides of the protein (Figure 2A). One of these channels is used for the binding of the CoA substrate, whereas the other is for binding carnitine. While the overall arrangement of the active site is similar to that in CAT (Figure 2E) and E2pCD (Leslie et al., 1988; Mattevi et al., 1993), there are significant differences in the binding modes of the substrates, especially CoA, as well as the catalytic mechanism, between CRAT and these other enzymes (see below).

The Carnitine Binding Site

The crystal structure of CRAT in complex with the substrate carnitine has been determined at 1.9 Å resolution (Table 1). The binding mode of carnitine is clearly defined by the crystallographic analysis (Figure 3A). We have also collected X-ray diffraction data on crystals of CRAT grown in the presence acetylcarnitine, the product of the reaction. The subsequent crystallographic analysis, at 1.9 Å resolution, showed however the presence of only carnitine in the active site (data not shown). This suggests that the acetylcarnitine has been hydrolyzed to carnitine during the crystallization process, and this hydrolysis may possibly be catalyzed by the enzyme itself.

Carnitine is bound in a partially folded conformation, with its carboxyl group pointed in the opposite direction from the hydroxyl group (Figure 3A). This bound conformation corresponds to one of the favored rotamers of this compound in solution, as indicated by NMR studies of free cartinine in aqueous solution (Colucci et al., 1986).

The carnitine binding site is formed by the β sheet (strands β11–β14) in the C domain and residues in α5–β1

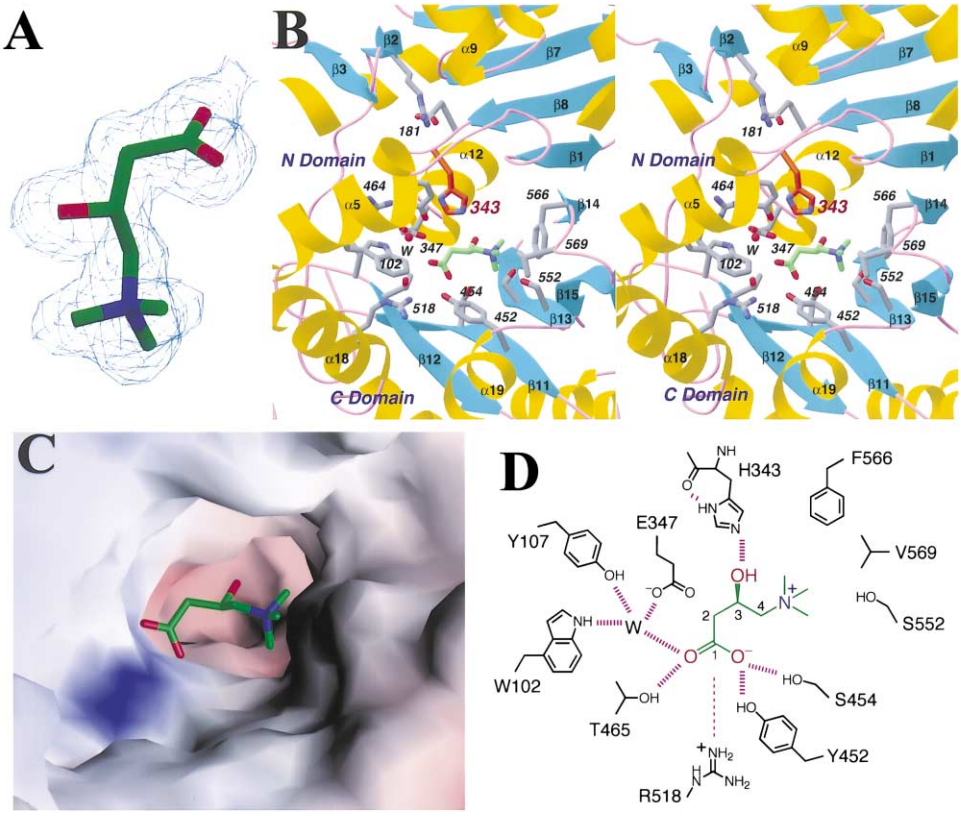

Figure 3. The Carnitine Binding Site of CRAT

(A) Final $2F_o–F_c$ electron density map for carnitine at 1.9 Å resolution. The contour level is at 1σ. Produced with Setor (Evans, 1993).

(B) Stereo diagram showing the carnitine binding site of CRAT. The side chain of the catalytic His343 residue is shown in red, and carnitine is shown in green. A water molecule that mediates carnitine binding is shown as a red sphere and labeled W. Produced with Ribbons (Carson, 1987).

(C) Molecular surface of CRAT in the region of the carnitine binding site. Produced with Grasp (Nicholls et al., 1991).

(D) Schematic drawing of the interactions between carnitine and CRAT. Hydrogen-bonding interactions are shown as thick dashed lines, and the electrostatic interaction between the carboxylate group and Arg518 is shown as the thin dashed line.

and β8–α12 in the N domain (Figure 3B). One face of the carnitine molecule is exposed to the solvent in the bound state (Figure 3C). The 3-hydroxyl group on carnitine forms a hydrogen bond with the side chain Nε2 atom of the catalytic His343 residue (Figure 3D), which has implications for the catalytic mechanism of this family of enzymes (see below). The structural analysis demonstrates that the catalysis is stereo-specific, as the other stereo-isomer of the hydroxyl group cannot maintain the same interactions with the enzyme.

The carboxylate group of carnitine has electrostatic interactions with the side chain guanidinium group of Arg518 (from helix α18), with a distance of about 4 Å, as well as a network of hydrogen-bonding interactions (Figures 3B and 3D). One of the carboxylic oxygen atoms is hydrogen-bonded to the side chain hydroxyls of Tyr452 and Ser454 (β11), whereas the other is hydrogen-bonded to the side chain hydroxyl of Thr465 (β12) and a water molecule. The tetrahedral coordination of this water is completed by three ligands from the enzyme, the Nε1 atom of Trp102 (α5), the Oη atom of Tyr107 (α5), and the Oε2 atom of Glu347 (β8–α12 loop), which also shield it from the solvent (Figure 3B).

The trimethylammonium group of carnitine is situated over the aromatic ring of the side chain of Phe566 (β14), with a separation of about 3.6 Å (Figure 3B). It is also close to the side chain of Ser552 (β13) and Val569 (β14–β15 loop). However, there are no negatively charged residues in the immediate vicinity of this group to balance its positive charge. Our structural analysis suggests this positive charge may be important for the catalytic activity of the enzyme (see below).

Most of the residues in this binding site are highly conserved among the carnitine acyltransferases (Figure 1). Our structural observations on the binding interactions of carnitine are supported by a large body of experimental data on mutants of these enzymes, as well as by the natural variations in the sequences of these enzymes (McGarry and Brown, 1997; Ramsay et al., 2001). For example, Thr465 and Arg518 have important roles in the recognition of the carboxylate group of carnitine (Figure 3D) and are conserved among all carnitine acyltransferases (Figure 1). However, these two residues are not conserved in the homologous choline acetyltransferases, because the choline substrate lacks a carboxylate group at this position (Cronin, 1997a). Moreover, the Arg→Asn mutation in bovine COT led to a 1650-fold increase in the K_m for carnitine, while having little effects

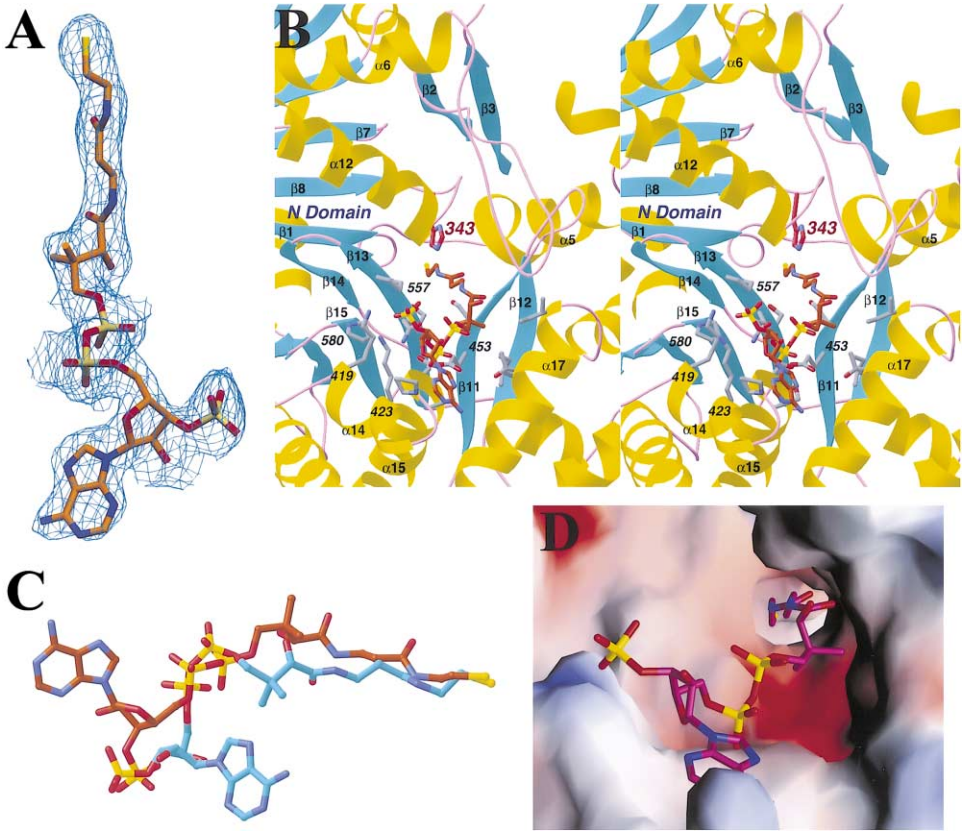

Figure 4. The CoA Binding Site of CRAT

(A) Final $2F_o–F_c$ electron density map for CoA at 2.3 Å resolution. The contour level is at 1σ. Produced with Setor (Evans, 1993).

(B) Stereo diagram showing the CoA binding site of CRAT. The CoA molecule is shown in brown. Produced with Ribbons (Carson, 1987).

(C) Overlap of the binding modes of CoA to CRAT (in brown) and CAT (in cyan).

(D) Molecular surface of CRAT in the region of the CoA binding site. (C and D) produced with Grasp (Nicholls et al., 1991).

on the K_m for CoA or the k_{cat} of the enzyme (Cronin, 1997a). Our structure shows an indirect, electrostatic interaction between this residue and the carboxylate group (Figure 3D), rather than a direct binding via hydrogen-bonding interactions.

In the binding site for the trimethylammonium group, Ser552 is the first residue of the strictly conserved STS motif among these acyltransferases (Figure 1). Mutation of this Ser residue to Ala in bovine COT produced a 17-fold increase in the K_m for carnitine, but only a 2-fold decrease in the k_{cat} of the enzyme (Cronin, 1997b), consistent with our structural observations (Figure 3B). Interestingly, mutation of the Thr residue in this motif to Ala produced a 90-fold increase in the K_m for carnitine, even though the side chain of this residue is pointed away from the active site. Detailed structural analysis showed that the side chain hydroxyl of the Thr residue is hydrogen-bonded to the main chain carbonyl oxygen of Tyr452 in strand β11 (Figure 3B), and the mutation may have disrupted the conformation of the enzyme in this area.

CRAT has a preformed binding site for the substrate carnitine. The only significant conformational difference in the active site between the free enzyme and the carnitine complex is in the side chain of Ser454, which adopts a different rotamer to have better hydrogen-bonding interactions with the carboxylate of carnitine (Figure 3D). Outside the active site, conformational differences are observed for several regions on the surface of the structure. In addition, there are small rigid body movements of the domains relative to each other. However, these changes are more likely due to flexibility in the enzyme or differences in crystal packing, and they have only minor impact on the active site region.

The CoA Binding Site

The crystal structure of CRAT in complex with the substrate CoA has been determined at 2.3 Å resolution (Table 1). To obtain this structure, X-ray diffraction data were collected on a crystal of the free enzyme of CRAT that was soaked overnight with 1.5 mM acetyl-CoA. The crystal suffered serious damage during the soak, giving rise to higher *R* factors for the diffraction data and the atomic model (Table 1). Nonetheless, the current data set is of sufficient quality to clearly define the binding mode of the substrate (Figure 4A). It also indicates that the compound bound in the active site is actually CoA (Figure 4A). This suggests that acetyl-CoA has been hydrolyzed to CoA during the overnight soaking process. Therefore, it appears that CRAT may be able to catalyze the hydrolysis of both acetylcarnitine and acetyl-CoA. We have also obtained cocrystals of the en-

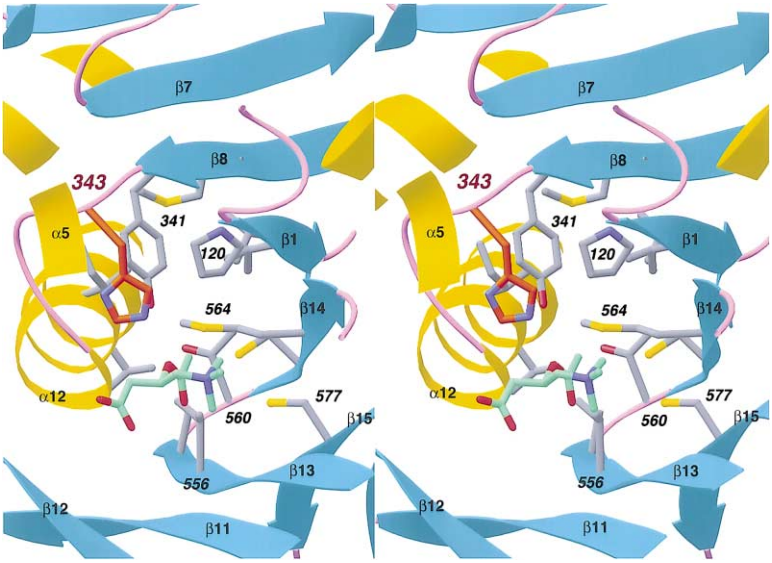

Figure 5. The Possible Fatty Acid Binding Site of Carnitine Acyltransferases

A model for the binding mode of acetylcarnitine is shown. The acetyl group points toward a hydrophobic pocket that could also be used to bind long chain acyl groups.

zyme with CoA. The subsequent crystallographic analysis revealed partial occupancy of the binding site. However, the binding mode of CoA confirms that observed from the soaked crystal.

The CoA binding site is on the opposite side of the His343 side chain from the carnitine binding site (Figure 2A). A special feature of the β sheet in the C domain is that the neighboring parallel strands β11 and β13 are splayed apart from each other at the C-terminal end (Figure 4B), which is also observed in CAT and E2pCD. This creates an opening between the two strands and allows the pantothenic arm of CoA to thread through it to reach the active site (Figure 4B). In the active site, the thiol group forms a hydrogen bond with the side chain Nϵ2 atom of the catalytic His343 residue.

The CoA molecule is bound in the fully extended, linear conformation (Figure 4B). The adenine base at one end of the molecule is about 25 Å from the thiol group at the other. This binding mode is in sharp contrast to the binding of CoA to CAT and E2pCD, where a folded conformation of CoA is observed (Leslie et al., 1988; Mattevi et al., 1993). A comparison of the two binding modes showed that the pantotheine portion has similar conformations, but the ADP portion has large differences (Figure 4C). The adenine bases are separated by about 14 Å in the two binding conformations. In CAT and E2pCD, the N1 and N6 atoms of the adenine base are hydrogen-bonded to the main chain amide and carbonyl of residues near the end of strand βI (Figure 2E). In CRAT, the equivalent residue, at the end of strand β15, is Pro580 (Figure 4B), which would abolish the type of interactions observed in CAT and E2pCD as it not only eliminates the hydrogen bond but also introduces steric clash with the adenine base. In our structure, the adenine base lies on the surface of the enzyme (Figures 5B and 5D) and there appears to be no specific recognition of its N1 or N6 atoms.

Residues in the CoA binding pocket are generally conserved among the carnitine acyltransferases (Figure 1). These include Lys419 and Lys423, which recognize the 3′-phosphate group of CoA (Figure 4B). In the binding site for the pantothenic arm of CoA, conserved residues Asp430 and Glu453 are directly hydrogen-bonded to each other (Figure 4B). Mutation of either residue can reduce the activity of the enzyme (Ramsay et al., 2001).

The Fatty Acid Binding Site

Our structures of the substrate complexes of CRAT also help to reveal the possible binding site for the hydrocarbon groups of long chain fatty acids in the CPTs. The acetyl group of acetylcarnitine, modeled based on the structure of the carnitine complex, points toward a hydrophobic pocket that is enclosed by the intersection of the two β sheets in the enzyme (strands β1 and β8 in the N domain, strands β13 and β14 in the C domain) and helix α12 (Figure 5). In CRAT, this pocket is partly filled by the side chain of Met564, coming from strand β14 (Figure 5). The equivalent residue in the CPTs is a glycine (Figure 1), which should make it possible for the hydrocarbon groups of the long chain fatty acid to bind in this pocket. The mutation of this Gly to Glu can cause L-CPT-I deficiency in patients (Ramsay et al., 2001). Additional differences in the amino acid sequences of CRAT and CPTs, for example in the α5–β1 region (Figures 1 and 3B), may also contribute to substrate binding in the CPTs.

Implications for the Catalytic Mechanism: Substrate-Assisted Catalysis

Our structures of the free enzyme and the substrate complexes of CRAT convincingly demonstrate the catalytic mechanism of this family of enzymes (Figure 6). The His residue in the active site acts as a general base in the catalysis (McGarry and Brown, 1997; Ramsay et al., 2001). It extracts the proton from the 3-hydroxyl group of carnitine or the thiol group of CoA, depending on the direction of the reaction. In our structures of the carnitine and CoA complexes, the reactive groups of both substrates are directly hydrogen-bonded to the His343 side chain. So the substrates are optimally positioned in our structures for the catalysis to happen. The activated hydroxyl or thiol group can then directly attack

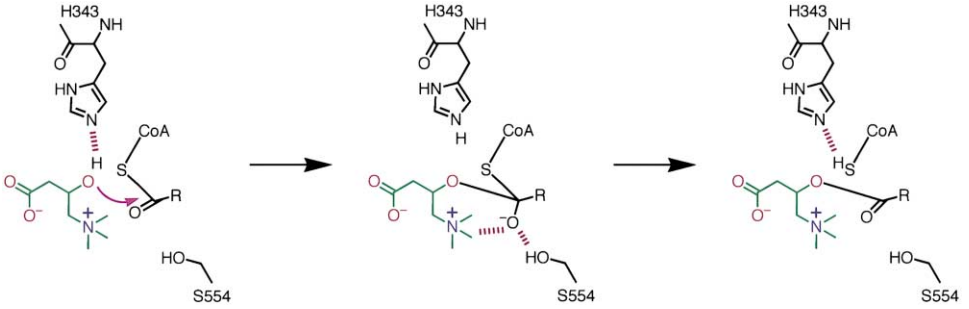

Figure 6. The Catalytic Mechanism of Carnitine Acyltransferases

The catalytic His343 residue can extract the proton from either carnitine or CoA. The oxyanion in the tetrahedral intermediate is stabilized by interactions with carnitine and the side chain hydroxyl of Ser554.

the carbonyl carbon in acyl-CoA or acylcarnintine, and the reaction proceeds without the formation of an acyl-enzyme intermediate.

It is also clear from the mechanism and our structures that if only acylcarnitine or acyl-CoA is bound in the active site, a water molecule binds in the opposite channel of the active site and can become the receptor for the acyl groups. Therefore, these transferases can also catalyze the simple hydrolysis of acylcarnitine or acyl-CoA, as we observed in our crystallization experiments. This futile hydrolysis is probably not a significant reaction in vivo, as the active site of the enzyme is likely to be occupied by its two substrates.

Structural analysis and modeling studies suggest that the trimethylammonium group of carnitine may play an important role in the catalysis by these acyltransferases, by stabilizing the oxyanion in the tetrahedral intermediate of the reaction (Figure 6). This suggests that carnitine acyltransferases may be an example of substrate-assisted catalysis (Dall'Acqua and Carter, 2000). Our structure model for the intermediate would place the oxyanion at about 3 Å distance to the trimethylammonium group of carnitine, suggesting strong, favorable interactions between the two charges (Figure 6). This is supported by the observation that the positive charge of carnitine is not critical for its binding, but is absolutely required for catalysis (Saeed et al., 1993). A carnitine analog, replacing the trimethylammonium group with the neutral *t*-butyl group, is not a substrate of the enzyme but can compete with carnitine for binding to the active site.

Based on our model for the tetrahedral intermediate, the oxyanion is also within 3 Å of the side chain hydroxyl of Ser554 (Figure 6). Mutation of this Ser residue, in the STS motif described earlier, produced a 10-fold decrease in the k_{cat} while having little impact on the K_m for carnitine (Cronin, 1997b). The equivalent Ser residue in CAT and E2pCD has also been identified as the oxyanion hole of those enzymes (Hendle et al., 1995; Lewendon et al., 1990). However, the small effect of the S554A mutation on the catalysis by COT also supports the functional role of the carnitine substrate itself in stabilizing the transition state of this reaction.

Disease-Causing Mutations

The crystal structure provides a molecular basis for understanding the effects of most of the natural and engineered mutations on these enzymes. A large number of natural mutations in these enzymes have been described, leading to various disease states (McGarry and Brown, 1997; Ramsay et al., 2001). These disease-causing mutations, as well as the engineered mutations, can be roughly divided into two categories, depending on whether they can affect (directly or indirectly) the active site of the enzyme. Mutations that directly affect the binding of carnitine or CoA have already been discussed here. The S113L mutation in CPT-II, one of the most common natural mutations in that enzyme, may indirectly affect the active site. The equivalent residue in CRAT is Ser99, located in helix α5 (Figure 1), which also contains residues (Trp102 and Tyr107) that have important roles in carnitine binding (Figure 3B). However, the side chain of this residue does not show strong interactions with other residues in the enzyme, which may be consistent with the fact the S113L mutation creates only mild effects (Ramsay et al., 2001).

Mutations in the second category may affect the stability or the production of the enzyme, as some of these mutants are known to have reduced cellular levels but with normal kinetic parameters (McGarry and Brown, 1997; Ramsay et al., 2001). A possible example of such a mutation is P50H in CPT-II, equivalent to Pro36 in CRAT and the first proline in the highly conserved LPXLPVP motif among these enzymes (Figure 1). The residue is located far from the active site, in the linker between helices α1 and α2 (Figure 2A). The mutation has only mild clinical effects (Ramsay et al., 2001), and the side chain of Pro36 is mostly exposed to the solvent (Figure 1).

For their important biological functions and as promising targets for the development of therapeutic agents against NIDDM and other human diseases, carnitine acyltransferases have received a significant amount of attention over the past years (Anderson, 1998; Giannessi et al., 2001; McGarry and Brown, 1997; Ramsay et al., 2001; Wagman and Nuss, 2001). Our structural information on these enzymes provides the foundation for understanding their catalytic mechanism and for structural-based design and optimization of their inhibitors.

Experimental Procedures

Protein Expression and Purification

Residues 30–626 of mouse carnitine acetyltransferase (CRAT) was subcloned into the pET28a vector (Novagen) and overexpressed in

E. coli at 20°C. The expression construct excluded the mitochondrial signal peptide (residues 1–29) of the native protein and introduced a hexa-histidine tag at the N terminus. The soluble protein was purified by nickel-agarose affinity chromatography, anion exchange, and gel filtration chromatography. The protein was concentrated to 40 mg/ml in a buffer containing 20 mM Tris [pH 8.5], 200 mM NaCl, and 10 mM DTT. The N-terminal His-tag was not removed for crystallization.

For the production of selenomethionyl proteins, the expression construct was transformed into DL41(DE3) cells. The bacterial growth was carried out in defined LeMaster media (Hendrickson et al., 1990), and the protein was purified using the same protocol as for the wild-type protein.

Protein Crystallization

Crystals of mouse CRAT free enzyme were obtained at 4°C by the sitting drop vapor diffusion method. The reservoir solution contained 100 mM Tris [pH 7.5] and 20% (w/v) PEG3350. The protein was at 20 mg/ml concentration (diluted 1:1 with water from the stock). The crystals were cryoprotected with the introduction of 25% (v/v) PEG200 and flash-frozen in liquid nitrogen.

Crystals of mouse CRAT in complex with carnitine were obtained at 4°C by the sitting drop vapor diffusion method. The reservoir solution contained 100 mM Tris [pH 8.0] and 12% (w/v) PEG3350. The protein was at 16 mg/ml concentration, and carnitine was present at 0.6 mM concentration.

For the CoA complex, crystals of the free enzyme of CRAT were soaked with 1.5 mM of acetyl-CoA overnight at 4°C before they are treated with PEG200 and flash-frozen for data collection.

Data Collection and Processing

X-ray diffraction data were collected on an ADSC CCD at the X4A beamline of Brookhaven National Laboratory. A seleno-methionyl single-wavelength anomalous diffraction (SAD) data set to 1.8 Å resolution was collected at 100K on the free enzyme crystal, and native reflection data sets were collected for the carnitine and CoA complexes. The diffraction images were processed and scaled with the HKL package (Otwinowski and Minor, 1997). The crystals belong to the space group *C*2, with cell dimensions of $a = 158.9$ Å, $b = 89.6$ Å, $c = 119.4$ Å, and $\beta = 127.5°$ for the free enzyme crystal; $a = 160.7$ Å, $b = 91.7$ Å, $c = 122.6$ Å, and $\beta = 128.8°$ for the carnitine complex; and $a = 162.3$ Å, $b = 92.0$ Å, $c = 122.9$ Å, and $\beta = 129.0°$ for the CoA complex. There are two molecules in the crystallographic asymmetric unit. The data processing statistics are summarized in Table 1.

Structure Determination and Refinement

The locations of 40 Se atoms were determined with the program SnB (Weeks and Miller, 1999) and further confirmed with SHELXS (Sheldrick, 1990). Reflection phases to 1.8 Å resolution were calculated based on the SAD data and improved with the program SOLVE (Terwilliger and Berendzen, 1999), which also automatically located 80% of the residues in both molecules. The atomic model was fit into the electron density with the program O (Jones et al., 1991). The structure of the carnitine complex was determined by molecular replacement with the program COMO (Jogl et al., 2001). The structure refinement was carried out with the program CNS (Brunger et al., 1998). The statistics on the structure refinement are summarized in Table 1.

Acknowledgments

We thank Randy Abramowitz and Craig Ogata for setting up the X4A beamline at the NSLS; Xiao Tao, Reza Khayat, Javed Khan for help with data collection at the synchrotron; and Andrew Leslie for the atomic coordinates of CAT:CoA complex.

Received: October 17, 2002
Revised: November 18, 2002

References

Abu-Elheiga, L., Matzuk, M.M., Abo-Hashema, K.A.H., and Wakil, S.J. (2001). Continuous fatty acid oxidation and reduced fat storage in mice lacking acetyl-CoA carboxylase *2*. Science *291*, 2613–2616.

Anderson, R.C. (1998). Carnitine palmitoyltransferase: a viable target for the treatment of NIDDM? Curr. Pharm. Des. *4*, 1–16.

Bieber, L.L. (1988). Carnitine. Annu. Rev. Biochem. *57*, 261–283.

Brunger, A.T., Adams, P.D., Clore, G.M., DeLano, W.L., Gros, P., Grosse-Kunstleve, R.W., Jiang, J.-S., Kuszewski, J., Nilges, M., Pannu, N.S., et al. (1998). Crystallography & NMR system: a new software suite for macromolecular structure determination. Acta Crystallogr. *D54*, 905–921.

Brunner, S., Kramar, K., Denhardt, D.T., and Hofbauer, R. (1997). Cloning and characterization of murine carnitine acetyltransferase: evidence for a requirement during cell cycle progression. Biochem. J. *322*, 403–410.

Carson, M. (1987). Ribbon models of macromolecules. J. Mol. Graph. *5*, 103–106.

Colucci, W.J., Gandour, R.D., and Mooberry, E.A. (1986). Conformational analysis of charged flexible molecules in water by application of a new Karplus equation combined with MM2 computations: conformations of carnitine and acetylcarnitine. J. Am. Chem. Soc. *108*, 7141–7147.

Cronin, C.N. (1997a). cDNA cloning, recombinant expression, and site-directed mutagenesis of bovine liver carnitine octanoyltransferase. Arg505 binds the carboxylate group of carnitine. Eur. J. Biochem. *247*, 1029–1037.

Cronin, C.N. (1997b). The conserved serine-threonine-serine motif of the carnitine acyltransferase is involved in carnitine binding and transition-state stabilization: a site-directed mutagenesis study. Biochem. Biophys. Res. Commun. *238*, 784–789.

Dall'Acqua, W., and Carter, P. (2000). Substrate-assisted catalysis: molecular basis and biological significance. Protein Sci. *9*, 1–9.

DiMauro, S., and Melis-DiMauro, P. (1973). Muscle carnitine palmitoyltransferase deficiency and myoglobinuria. Science *182*, 929–931.

Evans, S.V. (1993). SETOR: hardware lighted three-dimensional solid model representations of macromolecules. J. Mol. Graph. *11*, 134–138.

Giannessi, F., Chiodi, P., Marzi, M., Minetti, P., Pessotto, P., de Angelis, F., Tassoni, E., Conti, R., Giorgi, F., Mabilia, M., et al. (2001). Reversible carnitine palmitoyltransferase inhibitors with broad chemical diversity as potential antidiabetic agents. J. Med. Chem. *44*, 2383–2386.

Hendle, J., Mattevi, A., Westphal, A.H., Spee, J., de Kok, A., Teplyakov, A., and Hol, W.G.J. (1995). Crystallographic and enzymatic investigations on the role of Ser558, His610, and Asn614 in the catalytic mechanism of Azotobacter vinelandii dihydrolipoamide acetyltransferase (E2p). Biochemistry *34*, 4287–4298.

Hendrickson, W.A. (1991). Determination of macromolecular structures from anomalous diffraction of synchrotron radiation. Science *254*, 51–58.

Hendrickson, W.A., Horton, J.R., and LeMaster, D.M. (1990). Selenomethionyl proteins produced for analysis by multiwavelength anomalous diffraction (MAD): a vehicle for direct determination of three-dimensional structure. EMBO J. *9*, 1665–1672.

Holm, L., and Sander, C. (1993). Protein structure comparison by alignment of distance matrices. J. Mol. Biol. *233*, 123–138.

Jogl, G., Tao, X., Xu, Y., and Tong, L. (2001). COMO: A program for combined molecular replacement. Acta Crystallogr. *D57*, 1127–1134.

Jones, T.A., Zou, J.Y., Cowan, S.W., and Kjeldgaard, M. (1991). Improved methods for building protein models in electron density maps and the location of errors in these models. Acta Crystallogr. *A47*, 110–119.

Kerner, J., and Hoppel, C. (2000). Fatty acid import into mitochondria. Biochim. Biophys. Acta *1486*, 1–17.

Leslie, A.G.W., Moody, P.C., and Shaw, W.V. (1988). Structure of

chloramphenicol acetyltransferase at 1.75-Å resolution. Proc. Natl. Acad. Sci. USA *85*, 4133–4137.

Lewendon, A., Murray, I.A., Shaw, W.V., Gibbs, M.R., and Leslie, A.G.W. (1990). Evidence for transition-state stabilization by Ser-148 in the catalytic mechanism of chloramphenicol acetyltransferase. Biochemistry *29*, 2075–2080.

Lian, W., Govindasamy, L., Gu, Y., Kukar, T., Agbandje-McKenna, M., McKenna, R., and Wu, D. (2002). Crystallization and preliminary X-ray crystallographic studies on recombinant human carnitine acetyltransferase. Acta Crystallogr. *D58*, 1193–1194.

Mattevi, A., Obmolova, G., Schulze, E., Kalk, K.H., Westphal, A.H., de Kok, A., and Hol, W.G.J. (1992). Atomic structure of the cubic core of the pyruvate dehydrogenase multienzyme complex. Science *255*, 1544–1550.

Mattevi, A., Obmolova, G., Kalk, K.H., Teplyakov, A., and Hol, W.G.J. (1993). Crystallographic analysis of substrate binding and catalysis in dihydrolipoyl transacetylase (E2p). Biochemistry *32*, 3887–3901.

McGarry, J.D., and Brown, N.F. (1997). The mitochondrial carnitine palmitoyltransferase system. From concept to molecular analysis. Eur. J. Biochem. *244*, 1–14.

Nicholls, A., Sharp, K.A., and Honig, B. (1991). Protein folding and association: insights from the interfacial and thermodynamic properties of hydrocarbons. Proteins *11*, 281–296.

Otwinowski, Z., and Minor, W. (1997). Processing of X-ray diffraction data collected in oscillation mode. Meth. Enzymol. *276*, 307–326.

Ramsay, R.R., Gandour, R.D., and van der Leij, F.R. (2001). Molecular enzymology of carnitine transfer and transport. Biochim. Biophys. Acta *1546*, 21–43.

Saeed, A., McMillin, J.B., Wolkowicz, P.E., and Brouillette, W.J. (1993). Carnitine acyltransferase enzymic catalysis requires a positive charge on the carnitine cofactor. Arch. Biochem. Biophys. *305*, 307–312.

Sheldrick, G.M. (1990). Acta Crystallogr. *A46*, 467–473.

Terwilliger, T.C., and Berendzen, J. (1999). Automated structure solution for MIR and MAD. Acta Crystallogr. *D55*, 849–861.

Wagman, A.S., and Nuss, J.M. (2001). Current therapies and emerging targets for the treatment of diabetes. Curr. Pharm. Des. *7*, 417–450.

Weeks, C.M., and Miller, R. (1999). The design and implementation of SnB v2.0. J. Appl. Crystallogr. *32*, 120–124.

Accession Numbers

The Protein Data Bank accession number for the free enzyme structure is 1NDB, the carnitine complex is 1NDF, and the CoA complex is 1NDI.